



Influence of the parameters of a minimum quantity lubrication system on micro milling process results

Sonja Kieren-Ehse¹ · Tobias Mayer¹ · Benjamin Kirsch¹ · Jan C. Aurich¹

Received: 4 January 2023 / Accepted: 25 March 2023 / Published online: 11 July 2023
© The Author(s) 2023

Abstract

Micro end mills are characterized by high abrasive wear. To counteract this high abrasive wear, metalworking fluids can be applied. There are various methods to supply these fluids. One of these methods is the minimum quantity lubrication (MQL). The objective of this research is to investigate the influence of the supply direction and air pressure of a MQL system on the process result when micro milling. Micro milling tests were carried out using micro end mills made of cemented carbide with an effective diameter of 50 μm . When machining commercially pure titanium, the supply direction was varied at four levels relative to the feed direction (0° , 90° , 180° and 270°) and the air pressure at three levels (0.1 MPa, 0.2 MPa and 0.3 MPa). At each air pressure, the spindle speed was varied at three levels (30,000 rpm, 60,000 rpm, 120,000 rpm). Tool wear, surface quality, burr formation, and manufacturing accuracy were analyzed. In terms of the supply direction, the best results were obtained with a supply direction of 180° (in feed direction) — the lowest roughness and the most uniform slot bottom structure were machined. Regarding the influence of the supply direction on tool wear and manufacturing accuracy, no significant differences could be found. With regard to the air pressure, no clear result could be achieved. The influence of the spindle speed on the process results was higher than the influence of the air pressure. However, it is possible to select a suitable air pressure depending on the spindle speed.

Keywords Micro milling · Minimum quantity lubrication · Metalworking fluid · Tool wear · Surface roughness · Commercially pure titanium

1 Introduction

Micro products and microstructured surfaces can be found in many branches nowadays. These are, for example, medical technology, security technology, information technology and optics. Micro milling is a process that is well established for the manufacture of these products. Micro milling belongs to the mechanical micro machining processes, along with

processes such as micro drilling or micro grinding. It is characterized by its flexibility, as well as the variety of materials that can be machined [1], since it is not limited to electrically conductive materials, such as electrical discharge machining (EDM). In addition, micro milling is characterized by a high geometric freedom [1].

However, the process is accompanied by high abrasive wear, which limits tool life and the quality of the machining result [2]. The reason for the high wear is a significantly higher friction during cutting compared to conventional milling. The reason for the increased friction is the size effect, that the cutting edge radius is large compared to the chip thickness [2]. To exceed the minimum chip thickness, the cutting edge radius needs to be reduced or the chip thickness enlarged. When reducing the cutting edge radius, there is a physical limit due to the cutting tool material and it can not be reduced further, since the minimum achievable cutting edge radius depends on the cutting tool material used; the minimum cutting edge radius for cemented carbide tools approximately corresponds to the grain size of cemented

✉ Sonja Kieren-Ehse
sonja.kieren-ehse@mv.uni-kl.de

Tobias Mayer
tobias.mayer@mv.uni-kl.de

Benjamin Kirsch
benjamin.kirsch@mv.uni-kl.de

Jan C. Aurich
fbk@mv.uni-kl.de

¹ Institute for Manufacturing Technology and Production Systems, RPTU Kaiserslautern, Gottlieb-Daimler-Str., Kaiserslautern 67663, Germany

carbide. Furthermore, a large cutting edge radius to the chip thickness value has an influence on the process: for example, the chip formation and the process forces are negatively influenced [3]. In contrast, when increasing the chip thickness, there will be a risk of tool breakage due to the filigree structure of the micro end mills.

To counteract abrasive wear, tool coatings or metalworking fluids (MWF) can be applied. Tool coatings reduce the friction between tool and workpiece and improve the resistance to abrasive, adhesive, diffusive, and oxidation-related wear [4]. However, the cutting edge radius increases as a result of the applied coating [5].

When MWFs are used, there is no increase in the cutting edge radius. Their cooling and lubricating properties enable MWFs to reduce friction and remove the generated heat out of the contact zone. In conventional machining, the application of MWFs to reduce tool wear and thus increase tool life is state of the art. Initial investigations concerning the application of MWFs in micro milling also show a great potential, but the investigations are primarily limited to tool diameters bigger than 200 μm . Various cooling lubrication strategies were applied in the investigations. For instance, MQL [6] or flood lubrication [7], but also cryogenic [8] or gaseous cooling [9] were applied in micro milling. The most frequently used strategies in micro milling are flood lubrication and MQL. Marcon et al. [10] utilized a graphite nanoplatelet based lubricant when micro milling of H13 tool steel. The lubricant was applied via a nozzle with a diameter of 0.8 mm. It was shown that the use of the graphite nanoplatelet based lubricant reduces the tangential forces, but the dimensional accuracy deteriorates. Roushan et al. [11] compared dry machining, pure MQL, 0.25 vol% CuO and 1 vol% CuO nanofluid MQL in their research. They showed significant improvements in tool life and surface quality through the application of hybridized sustainable environments. Mittal et al. [12] compared the dry and the lubricated condition (flood lubrication) in micro milling of Ti6Al4V in their research. They showed that the cutting process forces could be significantly reduced by the application of MWF. Anand and Mathew [13] compared dry machining with MQL in micro milling Inconel 718, using sunflower oil as MWF. They showed that using MQL reduced burr height by 36%, burr width by 37%, and areal surface roughness by 32% compared to dry machining. Yang et al. [14] compared the cooling lubrication strategies flood cooling, MQL, and jet cold air with dry machining. They found out that the best results in terms of tool wear, surface roughness, and cutting force were achieved by using MQL. Biermann and Steiner [7] analyzed the influence of the lubrication methods MQL, flood lubrication and submerged machining on burr formation when micro milling. They found out that by using flood lubrication and submerged machining, the burr height can be reduced. Danish et al. [15] compared chilled air, MQL, and flood

cooling. They showed that MQL significantly reduced tool life and surface roughness compared to dry machining. The application of chilled air did not improve the results. Qu et al. [16] used three different MWFs in MQL and compared them to dry machining when micro milling Co40CrNiMo. They figured out that by using MQL compared to dry machining, tool wear, surface quality and mechanical properties of the workpiece are improved. Other authors investigated the influence of the parameters of the MQL systems on the process result when micro milling. Examples for these parameters are the supply direction of the MWF in relation to the feed direction, the air pressure applied to the system or the MWF quantity. Pham et al. [17] have chosen an alternative method for the supply of smallest quantities of MWF when micro milling Al 5052. They used a micropipette to apply a total quantity of lubricant of 20 μl and compared different MWFs. Their findings show that the best results were obtained with the high viscosity ionic liquid. Zheng et al. [18] considered the influence of supply direction and air pressure in MQL when micro milling Ti6Al4V and they compared their results to dry machining. The use of MQL significantly improved tool life. Regarding the parameters of the MQL system, the authors showed that the lowest surface roughness was achieved at air pressures of 0.15 MPa and 0.35 MPa and at the supply directions of 0 °C (against feed direction) and 180 °C (in feed direction). The lowest burr formation was achieved for the supply direction 270 °C. Vazquez et al. [19] also considered the influence of the supply direction (in feed direction and against feed direction) in MQL on the process result. The lowest tool wear was achieved for the supply of MWF in feed direction. With regard to burr height and surface roughness, similar results were obtained for both directions. Li and Chou [6] investigated the influence of oil volume flow rate and air flow rate when micro milling SKD61 steel. Among the considered oil flow rates of 1.88 mL/h, 3.75 mL/h and 7.5 mL/h and air flow rates of 25 L/min and 40 L/min, the best result was obtained with the lowest flow rate of 1.88 mL/h and an air flow rate of 40 L/min. In our own investigations, we considered oil flow rates of 0.7 mL/h, 1.5 mL/h and 6 mL/h for MQL in micro milling of commercially pure titanium [20]. The best results in terms of tool wear and surface quality were obtained at an oil flow rate of 0.7 mL/h.

In general, there are only a few studies in the literature on the influence of the parameters of MQL systems, especially for end mills with diameters smaller than 200 μm . Additionally, in many investigations, the parameters of the minimum quantity systems were kept constant: Ziberov et al. [21] applied an oil flow rate of 40.7 mL/h, an air pressure of 0.23 MPa, a supply direction of 0 °C (against feed direction), and a distance between nozzle and tool of 15 mm. Aslantas and Cicek [22] used an oil flow rate of 150 mL/h and an air pressure of 0.3 MPa. Hassanpour et al. [23] also only reported the oil flow rate of 240 mL/h and the air pressure

of 0.6 MPa. Kim et al. [24] have specified the oil flow rate of 10 mL/h, the air pressure of 0.15 MPa, and in addition the distance between nozzle and tool of 30 mm. Saha et al. [25] applied two MQL nozzles simultaneously in their investigations. These were placed behind the tool at 45 °C and – 45 °C [25]. Hence, there is still a demand for research on suitable MQL parameters for micro milling with ultra-small micro end mills to improve surface quality and tool life.

In the present study, the influence of supply direction and air pressure in combination with spindle speed on tool wear and surface quality in micro milling with tool diameters of 50 µm was investigated.

2 Machining setup and measurement technology

2.1 Tools and workpiece material

For the investigation of the influence of the supply direction and the air pressure of the minimum quantity system, uncoated micro end mills with a diameter of 50 µm were used. The micro end mills were developed at the Institute for Manufacturing Technology and Production Systems at the RPTU Kaiserslautern. They are single edged with an axial rake angle of 0 °C, an axial clearance angle of 20 °C and a minor cutting edge angle of 12 °C (see Fig. 1 c). Further information about the tools can be found in references [26, 27]. The micro end mills were manufactured on a LT Ultra MTC-250 ultraprecision turning machine and made of fine grain cemented carbide (PN90 by Sandvik¹: 91% WC and 9% Co, grain size 0.2 µm). The cutting edge radii of the micro end mills were measured with an atomic force microscope (NaniteAFM, Nanosurf¹) after tool manufacture and are about 200 nm. For further details regarding the measurement setup, see reference [28].

The workpiece material used for the investigations was cp-titanium grade 2, which was delivered in the form of sheet metal. Samples with a size of 25 mm x 75 mm x 2 mm were cut out for the investigations. The chemical composition is listed in Table 1.

2.2 Experimental setup and process parameters

The micro milling tests were conducted on a precision milling machine developed at the Institute for Manufacturing Technology and Production Systems at the RPTU Kaiserslautern. The precision milling machine is a desktop sized machine tool built up on a granite machine bed. The machine tool

consists of three linear axes (X, Y and Z). The working table is mounted on the X- and Y-axis (ball screw bearing), which have a feed travel of each 100 mm. The Z-axis (cross roller bearing) has a feed travel of 60 mm. On this axis a 3R¹ palletizing system is installed positioning the main spindle in the machine tool. An ABL¹ MM160 air bearing spindle was used (spindle speed range: 20,000 rpm–160,000 rpm).

The investigation is divided into two test series: The investigation of the influence of the supply direction of the MWF in relation to the feed direction and the investigation of the influence of the air pressure. The experimental setup for both test series is identical and shown in Fig. 1 a). The specimen holder with the titanium sample is fixed on the working table.

The supply of the MWF is realized by using a nozzle based on the Venturi principle for MQL. The parameters of the system are the MWF quantity and the applied air pressure. The influence of the MWF quantity has already been investigated in a preliminary study by the authors, the influence of the applied air pressure on the process results is one of the subjects of the present investigation. The investigation on the influence MWF quantity considered the influence of three different MWF quantities (0.7 mL/h, 1.5 mL/h, 6.0 mL/h) compared to dry machining on the tool wear and surface roughness [20]. The best results were obtained with the lowest oil flow rate investigated, hence an oil flow rate of 0.7 mL/h was chosen in the present study. The second subject of the present study is the influence of the supply direction of the MWF in relation to the feed direction. For defined adjustability of the supply direction, a holder with four insert positions for the MQL nozzle was attached to the main spindle. The insert positions are positioned at 90 °C intervals around the circumference. In addition, the insert positions define the angle between the nozzle and the specimen surface as 30 °C and the distance between the nozzle and the micro end mill of 10 mm. The MQL nozzle is supplied with compressed air and MWF by tubes. The blue tube in Fig. 1 a) is the supply tube for the MWF, which is connected to the MWF reservoir (MWF: DiaMond80 (oelheld¹); specifications, see Table 2) that is placed on the machining table. The applied compressed air (black tube) is controlled by the compressed air control unit (see Fig. 1 d). This consists of a shut-off valve, a pressure reducer, and a pressure gauge. This system enables the setting of pressures between 0.05 MPa and 0.6 MPa in steps of 0.001 MPa. An observation camera is integrated in the precision milling machine for process monitoring.

In the first test series, four different supply directions of the MWF in relation to the feed direction were investigated. The directions were 0°, 90°, 180° and 270°, whereby 0° corresponds to feed direction of the workpiece. The feed direction of the workpiece was kept constant for all tests in positive Y-direction to exclude for example an influence of the tilt of the main spindle on the process results. The pressure was kept constant at 0.3 MPa and 60,000 rpm was

¹ Naming of specific manufacturers is done solely for the sake of completeness and does not necessarily imply an endorsement of the named companies nor that the products are necessarily the best for the purpose.

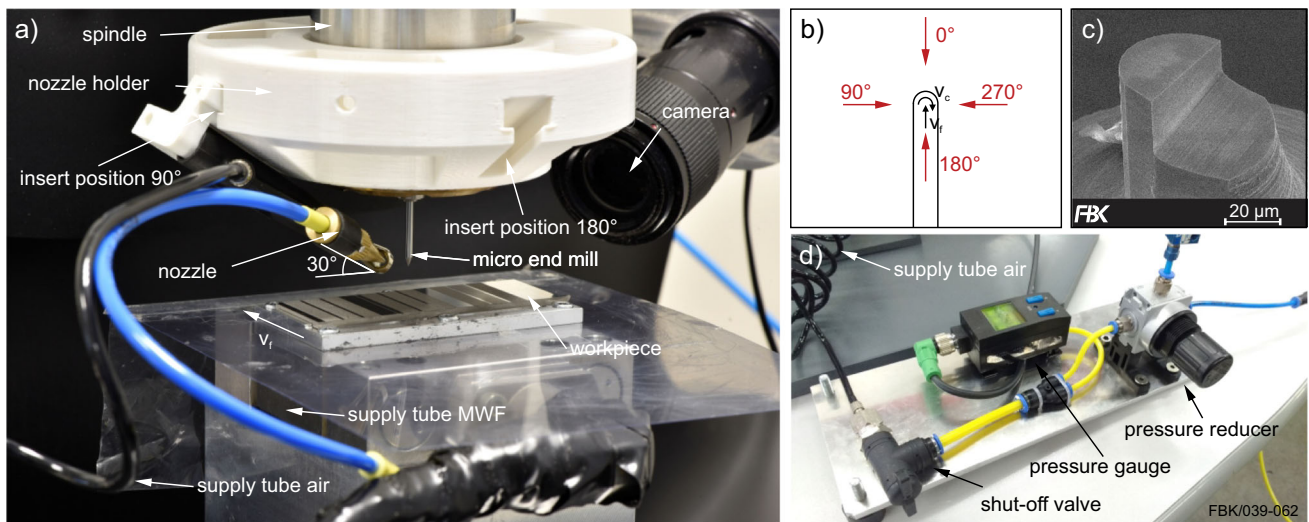


Fig. 1 a) Experimental setup, b) Definition of the supply directions, c) New micro end mill $d=50\ \mu\text{m}$, d) Compressed air control unit

used as the spindle speed. Figure 1 b) shows the definition of the four directions considered and Table 3 summarizes the experimental conditions of the first test series. Table 4 gives an overview about the experimental design.

The aim of the second test series was the investigation of the influence of the supply pressure of the air. The air pressure was varied on three levels (0.1 MPa, 0.2 MPa, 0.3 MPa) and the spindle speed also on three levels (30,000 rpm, 60,000 rpm, 120,000 rpm). The run-out of the spindle was measured with two capacitive sensors (Typ C23-C, Lion Precision¹). A maximum run-out of $1.3\ \mu\text{m}$ was measured at each of the three spindle speeds used. The spindle speed of 90,000 rpm was not used due to its poor run-out (max. $1.6\ \mu\text{m}$). The best direction obtained from the first test series was used as supply direction of the MWF. Table 5 summarizes the experimental conditions of the second test and Table 6 the experimental design.

For both test series the depth of cut of $5\ \mu\text{m}$, the feed travel of 1000 mm and the feed per tooth of $1\ \mu\text{m}$ were kept constant.

2.3 Measurement technology and evaluation methodology

After micro milling, confocal microscope images of the slots were taken using a Nanofocus¹ OEM microscope

Table 1 Chemical composition of cp-titanium grade 2 (manufacturer specifications)

	Ti	Fe	O	N	C	H
max. wt. (%)	Base	0.05	0.135	0.009	0.005	0.0006

(camera resolution: 1200×1200 ppi) with a 60x objective lens (numerical aperture 0.9). The measuring field was $268\ \mu\text{m} \times 523\ \mu\text{m}$, resulting from two stitched single images. The first measurement was done in the middle of the first milled slot (after 12.5 mm), further measurements were carried out at intervals of 100 mm. Out of these ten measurements the arithmetic mean roughness R_a (Gaussian filter: $8\ \mu\text{m}$) and the arithmetic mean height S_a were evaluated. R_a was evaluated along a profile section for a length of $400\ \mu\text{m}$ in the middle of each slot, S_a for a field with a length of $400\ \mu\text{m}$ and a width of 90% of the slot width. To evaluate the manufacturing accuracy, the slot width and slot depth were considered. The slot width was determined via a profile section perpendicular to the feed direction and the slot depth via the difference between the plane of the slot bottom and the plane of the face-milled surface for each measurement. The burr formation was qualitatively evaluated using confocal microscope images of the first slot (12.5 mm feed travel).

After micro milling, scanning electron microscopy (SEM) images of the tools were taken using a FEI¹ Quanta 600 after micro milling to evaluate tool wear. The working distance was 12 mm and the acceleration voltage 20 kV (SE).

Table 2 MWF manufacturer specifications

MWF	DiaMond80
kinematic viscosity at $40\ ^\circ\text{C}$	$2.0\ \text{mm}^2/\text{s}$
density at $15\ ^\circ\text{C}$	$0.78\ \text{g}/\text{cm}^3$
flashpoint	$82\ ^\circ\text{C}$

Table 3 Experimental conditions test series 1: influence of the supply direction on the process results

machining condition	spindle speed	60,000 rpm
	feed per tooth	1 μm
	depth of cut	5 μm
	feed travel	1000 mm
MQL condition	oil flow rate	0.7 mL/h
	air pressure	0.3 MPa
	MWF	DiaMond80
	distance	10 mm
	nozzle angle	30°
micro end mill	tool diameter	50 μm
	cemented carbide	
	single edged	
workpiece	cp-titanium	grade 2

Table 5 Experimental conditions test series 2: influence of the air pressure and spindle speed on the process results

machining condition	feed per tooth	1 μm
	depth of cut	5 μm
	feed travel	1000 mm
MQL condition	supply direction	180°
	oil flow rate	0.7 mL/h
	MWF	DiaMond80
	distance	10 mm
micro end mill	nozzle angle	30°
	tool diameter	50 μm
	cemented carbide	
workpiece	single edged	
	cp-titanium	grade 2

3 Results and discussion

The following section is divided into the two test series: the investigation of the influence of the supply direction of the MWF in relation to the feed direction and the investigation of the influence of the supply pressure of the air.

3.1 Supply direction of the metalworking fluid

3.1.1 Tool wear

Figure 2 shows the tool wear depending on supply direction after a feed travel of 1000 mm. The SEM images show one representative tool per supply direction. No tool breakage occurred before the feed travel of 1000 mm was reached.

The comparison of the tool wear as a function of the supply direction only shows slight direction dependent changes in wear patterns. The tool wear of the 0° and 90° direction is characterized by built-up edge formation and adhesions in the region of the cutting edge corner. Abrasive wear or smaller breakouts cannot be ruled out, as they would be completely covered by the built-up edge. The tools of the 180° supply direction show adhesion in the area of the circumferential cutting edge, rake face and flank face. In addition,

slight abrasive wear is visible. The images of the 270° supply direction show a built-up edge in the area of the cutting edge corner, as it was already visible for the 0° and 90° supply direction. Concluding, no best or worst direction can be given regarding the influence of the supply direction, as the differences in wear are small.

3.1.2 Surface

The surface at the slot bottom is evaluated quantitatively based on the surface roughness of the slot bottom and qualitatively based on the surface structure of the slot bottom after a feed travel of 12.5 mm (middle of the first slot). Figure 3 shows the surface roughness Ra and Sa as a function of the supply direction.

The lowest Ra value with 79.9 nm was achieved by using the supply direction 180° (in feed direction). This agrees to the results by Zheng et al. [18] and Vazquez et al. [19] that a low surface roughness (Ra) was achieved by using the supply direction 180°. However, both also reached similar low Ra values under the supply direction 0° which contrasts with the results obtained in this study. Using the supply directions 0° and 270° resulted in the highest Ra values (99.7 nm and 102.7 nm). Furthermore, the standard deviation at 0° is more

Table 4 Experimental design test series 1: influence of the supply direction on the process results

factor	levels			
	0°	90°	180°	270°
supply direction				
full factorial design size	4			
design repetitions	3			
total number of runs	12			

Table 6 Experimental design test series 2: influence of the air pressure and spindle speed on the process results

factor	levels		
air pressure / MPa	0.1	0.2	0.3
spindle speed / krpm	30	60	120
full factorial design size	9		
design repetitions	3		
total number of runs	27		

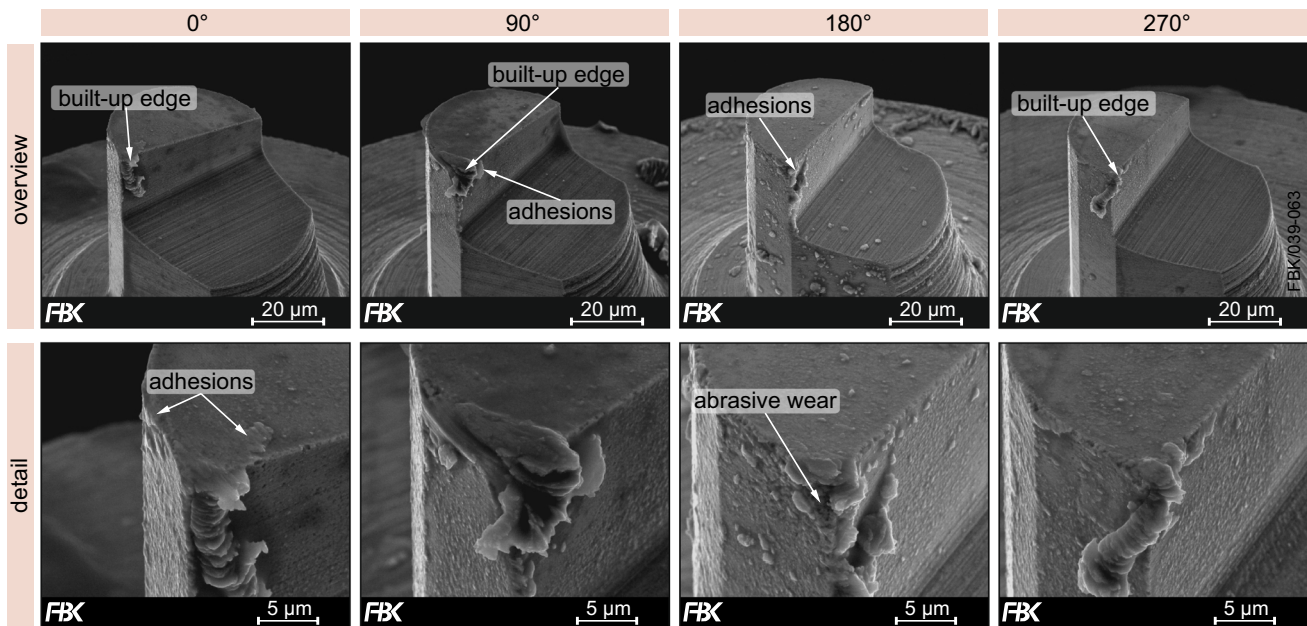


Fig. 2 Wear of micro end mills after a feed travel of 1000 mm depending on supply direction

than twice the value compared to those at 270° (36.7 nm vs. 14.4 nm). Overall, the Ra values deteriorated in the order 180°, 90°, 0°, 270°. This order clearly shows the influence

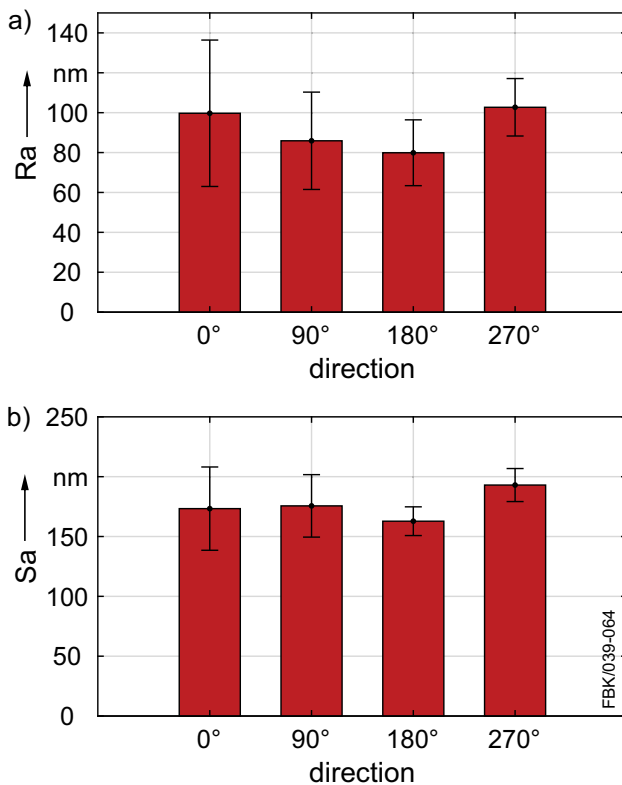


Fig. 3 Surface roughness results depending on supply direction: a) Ra values, and b) Sa values

of the contact conditions of the tool on the process results during full slot milling in combination with the supply direction of the MWF. At supply direction of 180°, the spraying direction of the MWF is in the same direction as the feed direction of the tool, which means that the MWF is permanently supplied to the current end of the slot and thus to the contact zone of the machining process. In addition, the rotary motion of the micro end mill pushes the MWF into the contact zone. At the angles of 90°, 0° and 270°, the previously micro milled step (depth of cut) hides the contact zone, representing a kind of wind trap. This results in an area for each nozzle angle that can only be wetted indirectly with MWF. Indirect wetting is possible for example when the tool pulls the MWF into the contact zone. The effect of the wind trap is additionally reinforced by the high burr formation. This effect was first described for micro milling by Saha et al. [29]. They called this area, which is hidden during micro milling, shadow zone. The zone increases with the axial depth of cut and the top-burr height. Compared to conventional milling, micro milling generates much more burr in relation to the tool diameter or the depth of cut. Especially when machining cp-titanium, a lot of burr is formed during the machining process, with the up-milling side having less burr compared to the down-milling side. The burr formed during machining additionally covers the contact zone and thus shields it from MWF. This shielding is most pronounced on the down-milling side (270°). This explains why in the present investigation the results for 0° are not as good as in the investigations of [19]. In their investigations the burr height for 0° and 180° was almost the same [19], which meant that the contact zone could be reached by the MWF

for both directions. Besides the influence of the workpiece (machined slot, burr), the micro end mill has an influence on the accessibility of the contact zone. In the order of 90° , 0° , 270° the area increases in which the back of the tool is mainly sprayed during material separation whereby the tool covers the contact zone.

The influence of the supply direction of the MWF on the surface roughness due to the shielding of the contact zone by burr formation or the accessibility of the contact zone by the MWF depending on the supply direction is also shown by the S_a values (Fig. 3 b). However, the differences are less pronounced here. The best result with 162.8 nm was achieved at 180° , the worst with 193.0 nm at 270° .

The surface structures shown in Fig. 4 provide information in how far the surface roughness differed and what led to the increase in R_a and S_a values.

The surface structures on the slot bottom show differences depending on the supply direction, with the largest difference being visible for the 0° supply direction. In the 0° supply direction, the kinematics of face milling are not recognizable, but a structure characterized by built-up edges. The scratches created by the rotary motion do not form circles due to the built-up edges, but have a more angular shape. Irregular deposits of the built-up edge at the slot bottom result in high roughness values and strongly fluctuating roughness values, which can be seen in particular in the R_a values and also in the rising standard deviations. The slot bottom structures of the 90° , 180° and 270° supply directions do not indicate built-up edge formation. The most regular structure was obtained under a supply direction of 180° , which also showed the lowest roughness values.

Figure 5 shows the burr formation depending on the supply direction.

The biggest difference in burr formation can be seen between the supply directions 0° , 90° and 180° compared with the supply direction 270° . At 0° , 90° and 180° , there is clearly more burr on the down-milling side, while there is hardly any burr on the up milling side. Similar results were obtained for example by Aslantas et al. [30] and Kiswanto et al. [31]. This agrees with the results of Vazquez et al. [19] that the burr formation results are similar for 0° and 180° . Compared to the other directions, the burr width and height at 270° is smaller on the down-milling side, but the burr width on the up milling side is larger. The burr shape also differs on the up milling side compared to 0° , 90° and 180° . The reason for this is the supply direction. With a supply direction of 270° , the MWF is sprayed onto the contact zone from “the direction of the down-milling side”. This cools and lubricates especially the point where the micro end mill exits the material, resulting in a lower temperature and less burr formation. The up milling side, on the other hand, is almost not reached at all with this supply direction. This results in a dif-

ferent burr formation and shapes due to the locally different cooling lubrication.

Overall, the best results were obtained with a supply direction of 180° . With this supply direction, the lowest roughness values and the most uniform slot bottom structure were achieved, which indicates better cooling lubrication compared to the other supply directions. For this reason, the 180° supply direction was selected for the second test series and further investigations.

3.1.3 Manufacturing accuracy

An important criterion for the usability or functionality of micro components or microstructured surfaces is the manufacturing accuracy. For the manufactured structures, this was evaluated based on the resulting slot width and depth (compared to the set ones). The results are depicted in Fig. 6.

The nominal diameter of the tools used was $50\ \mu\text{m}$ and the width of the rake face $47\ \mu\text{m}$. The difference between these two values is the clearance needed when using single-edged micro end mills to avoid unwanted contact between the micro end mill and the workpiece. This contact would result in immediate tool breakage. Based on this information as well as the run-out of the spindle or the clamping error of the tool of up to $2\ \mu\text{m}$, slot widths of about $48\ \mu\text{m}$ to $52\ \mu\text{m}$ are possible, which are not attributable to material separation. Deviations beyond this range are either due to tool wear or built-up edge formation. Figure 6 a) shows that all mean values are within this range. However, the mean value of 0° is at the lower limit, so that the standard deviation exceeds the lower limit of the range.

Similar to the slot width, for the slot depth a range can be indicated in which the slot depths should be without considering the influence of the material separation. The depth of cut was set to $5\ \mu\text{m}$. After face milling (planning), the surface needs to be optically touched with the micro end mill to set the zero point on the surface in the Z direction. This can be done with an accuracy of lower than $0.5\ \mu\text{m}$. Thus, the zero point is maximally between the real surface and $0.5\ \mu\text{m}$ below the real surface. Another point that influences the accuracy is the roughness of the face-milled surface, since roughness peaks lead to premature touching before the surface is reached. To determine a maximum value for this, the maximum peak height of the scale limited surface S_p of the face-milled surface was determined. The maximum peak height of the scale limited surface is $S_p = 0.42\ \mu\text{m} \pm 0.12\ \mu\text{m}$. Thus, a maximum deviation of approx. $0.5\ \mu\text{m}$ can occur due to the roughness peaks. As with the slot width, all mean values are within the range of $4.5\ \mu\text{m}$ to $5.5\ \mu\text{m}$ (see Fig. 6 b). It is only the standard deviation of 90° that exceeds this range.

Overall, no significant influence of the feed direction on the manufacturing accuracy can be detected. Only the slot

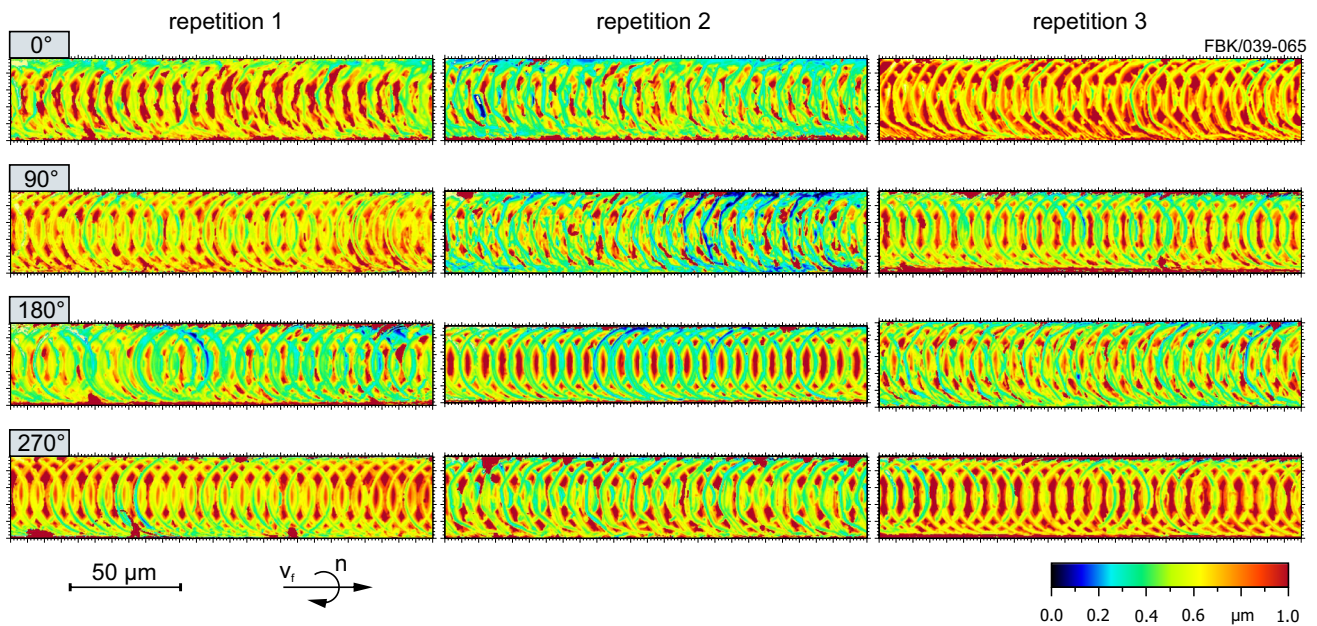


Fig. 4 Slot bottom topography after a feed travel of 12.5 mm depending on supply direction

width at 0° and the slot depth at 90° show slight deviations from the nominal values. Vazquez et al. [19] came to a contrary conclusion: the best result for the slot width was achieved for 0° direction. However, this deviation from the present study for the 0° direction can be explained by the poor accessibility of the contact zone by the cooling lubricant due to the strong burr formation of commercially pure titanium.

3.2 Air pressure

Besides the supply direction of the MWF in relation to the feed direction, the air pressure is another influencing factor for MQL. Since the nozzle exit speed also changes with the applied air pressure, the spindle speed was also varied on three levels in addition to the air pressure in this test series. With the aid of this analysis, a possible correlation between air pressure and spindle speed or cutting speed can be investigated.

First, the spray characteristics of the MQL system were determined. For this purpose, a sheet of paper was sprayed with blue colored MWF for 1 s. This was carried out for the three pressures 0.1 MPa, 0.2 MPa, and 0.3 MPa at a constant distance between nozzle and sheet of paper of 10 mm and a constant oil flow rate of 0.7 mL/h. The result of the characterization is shown in Fig. 7. This confirms the relationship described in the literature that there is a reduction in droplet size with increasing air flow rate or air pressure [6]. At an air pressure of 0.1 MPa, few but larger marks of the droplets can be seen. With increasing air pressure, the droplet size decreases, and the number of droplets increases.

3.2.1 Tool wear

Figure 8 shows the tool wear after a feed travel of 1000 mm depending on air pressure and spindle speed. For each parameter combination, a tool is exemplarily shown which has withstood the feed travel of 1000 mm without tool breakage.

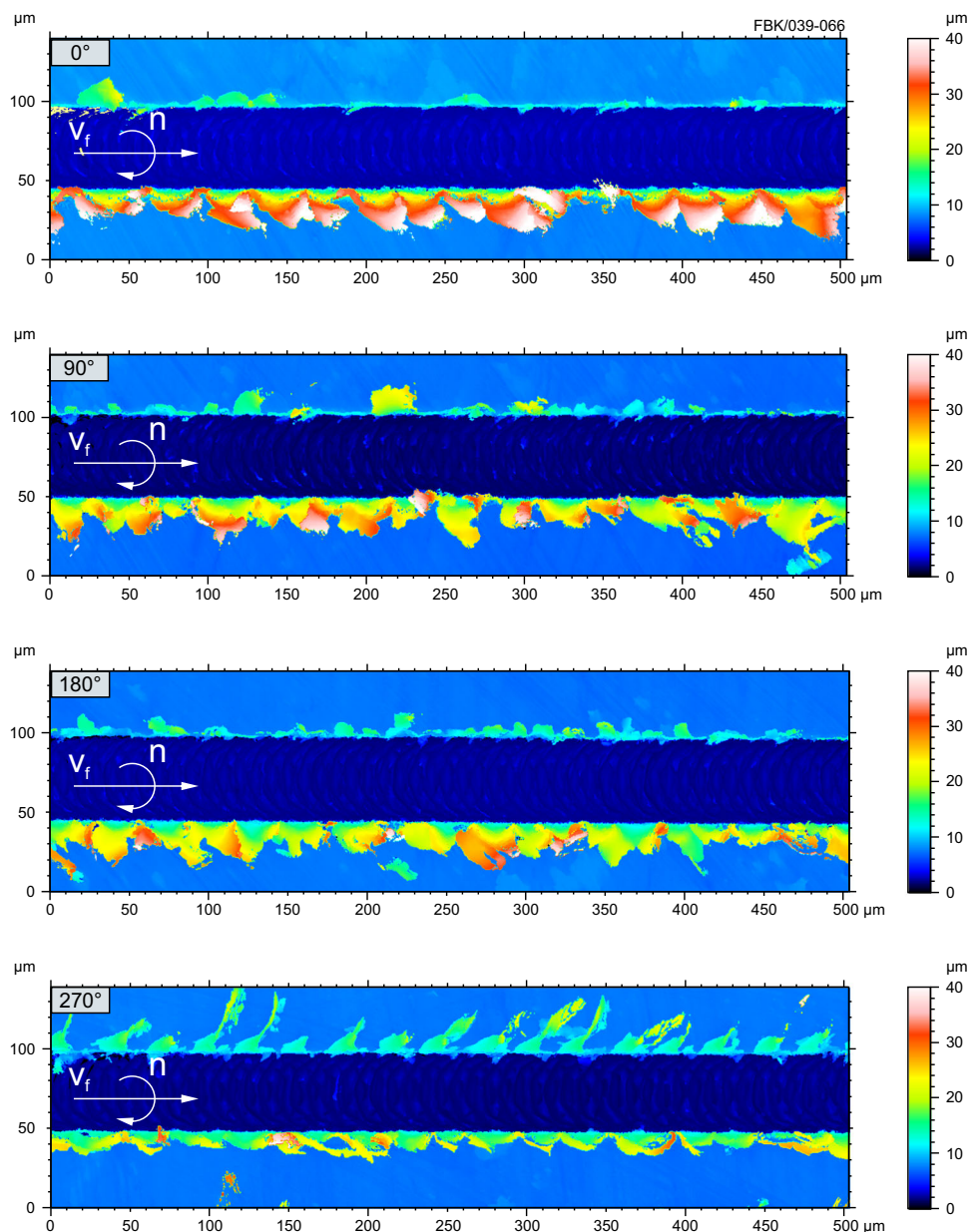
When machining at 30,000 rpm and 60,000 rpm, the tool wear shows a similar result independent of the air pressure. All tools are characterized by slight adhesions or small built-up edges in the region of the cutting edge corner. At a spindle speed of 120,000 rpm the tools applied at an air pressure of 0.1 MPa or 0.2 MPa show a similar wear pattern. Only at a pressure of 0.3 MPa the tool wear deviates from the other wear patterns, as a breakout occurred here. When using this parameter combination, tool breakage occurred after a feed travel of 550 mm or 150 mm for the other two tools. Small oil droplets, such as those present at 0.3 MPa (see Fig. 7), result in more heat being removed from the contact zone by evaporation [6]. Cooling the softened material too quickly could have led to the breakout or the tool fractures. This leads to the conclusion that this combination can be classified as unsuitable with regard to tool wear. The influence of the other parameters on wear is small.

3.2.2 Surface

The quantitative evaluation of the roughness at the slot bottom is depicted as a function of the air pressure and the spindle speed using the parameters R_a and S_a , see Fig. 9.

The analysis of the R_a values shows that the values vary greatly depending on the air pressure and spindle speed

Fig. 5 Burr formation after a feed travel of 12.5 mm depending on supply direction



applied. Thereby, the lowest mean value was obtained with 36.1 nm at a pressure of 0.2 MPa and a spindle speed of 30,000 rpm and the highest mean value resulted with 103.6 nm at a pressure of 0.3 MPa and a spindle speed of 60,000 rpm.

In general, the influence of the spindle speed on the mean values is large. This is due to higher temperatures in the cutting zone at higher cutting speeds [32]. The Ra values when using the spindle speed of 60,000 rpm are at a high level in a range between 88.7 nm and 103.6 nm, and the Ra values for the spindle speed 120,000 rpm are at a low level (40.7 nm–49.8 nm). At these speeds, the air pressure used has only a minor influence on the mean values of Ra. This indicates that at these spindle speeds the influence of heat

input when micro milling is greater than the effect of cooling lubrication. All three pressures considered resulted in insufficient cooling lubrication. In comparison, for the spindle speed 30,000 rpm, a large influence of the air pressure applied on the mean values of Ra can be observed. The lowest mean value at this spindle speed is 36.1 nm at 0.2 MPa and the highest at 0.3 MPa is 76.6 nm which is more than twice the value of 0.2 MPa. The mean value for the air pressure of 0.1 MPa is 53.7 nm, which is between the values of 0.2 MPa and 0.3 MPa. In contrast to the other two spindle speeds, at 30,000 rpm it can be seen that the contact zone is lubricated differently depending on the pressure. One reason may be the different droplet size, number and velocity as a function of pressure: At 0.1 MPa, the contact zone is impacted by a

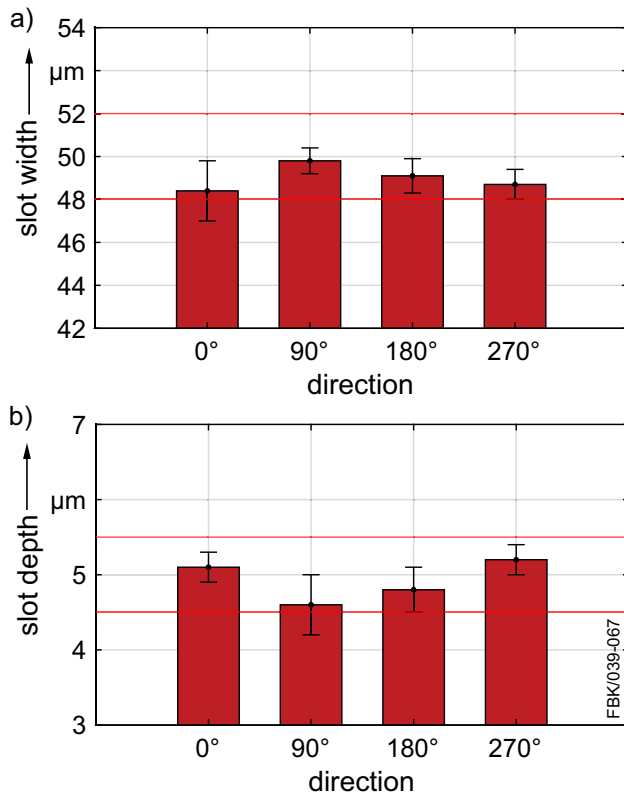


Fig. 6 Manufacturing accuracy results depending on supply direction: a) slot width, and b) slot depth

smaller number of larger droplets at a lower velocity compared to the higher pressures (see Fig. 7). Due to the small number, it is probably the case that only one droplet hits the contact zone from time to time, resulting in insufficient cooling lubrication. At 0.3 MPa, the higher velocity of the droplets is probably the limiting factor: due to the high velocity of the droplets or the aerosol, enough MWF (many small droplets) is transported to the contact zone, but the velocity forces it out of the contact zone again.

Compared to the Sa values at a spindle speed of 60,000 rpm, the average values at the spindle speeds of 30,000 rpm and 120,000 rpm fluctuate significantly more (see Fig. 9 b). At a spindle speed of 120,000 rpm, the level of the mean values of the Sa values differs from the Ra values. For Ra values, the

mean values were at a low level at 120,000 rpm. The Sa values at 120,000 rpm are at a similar level compared to the spindle speed 60,000 rpm. The qualitative trend for the spindle speed of 120,000 rpm corresponds to the distribution of Ra values. The low Sa value of 138.8 nm at an air pressure of 0.3 MPa can be explained by tool breakouts and the associated strong rounding of the cutting edge, as well as the increased built-up edge formation due to the breakage. The constantly changing geometry of the cutting edge resulting from these aspects is also indicated by the high standard deviation of the Ra value at 120,000 rpm and 0.3 MPa.

Concluding, no clear result could be achieved with regard to the best air pressure. The influence of the spindle speed on the process results was higher than the influence of the air pressure. However, the following conclusions can be drawn: With the spindle speed of 30,000 rpm, the best results were obtained at an air pressure of 0.2 MPa. No statement can be done concerning the spindle speed of 60,000 rpm. At the spindle speed 120,000 rpm and an air pressure of 0.2 MPa, a slightly worse roughness was achieved compared to 0.1 MPa. 0.3 MPa has already been identified in tool wear as a pressure that should be avoided.

3.2.3 Manufacturing accuracy

In contrast to the results of manufacturing accuracy for the supply direction, there are differences observable depending on the air pressure or the spindle speed, see Fig. 10.

Figure 10 a) shows that, with the exception of “30,000 rpm-0.1 MPa”, “60,000 rpm-0.2 MPa”, and “120,000 rpm-0.3 MPa”, all mean values are within the nominal range of 48 μm to 52 μm. Taking the standard deviation also into account, only the parameter combinations “30,000 rpm-0.2 MPa”, “30,000 rpm-0.3 MPa”, and “60,000 rpm-0.3 MPa” are in this range. The mean value of the slot width at 30,000 rpm-0.1 MPa, which is slightly below 48 μm, can be explained by a slight tool wear at the cutting edge corner. However, since the cutting edge corner is covered by adhesions after machining (see Fig. 8), this cannot be proven by the SEM images. The mean values of slot widths above 52 μm (“60,000 rpm-0.2 MPa”, and “120,000 rpm-0.3 MPa”) can be attributed to built-up edge formation. This is consis-

Fig. 7 Spray characteristics of the MQL system as a function of air pressure at a distance of 10 mm and an oil flow rate of 0.7 mL/h

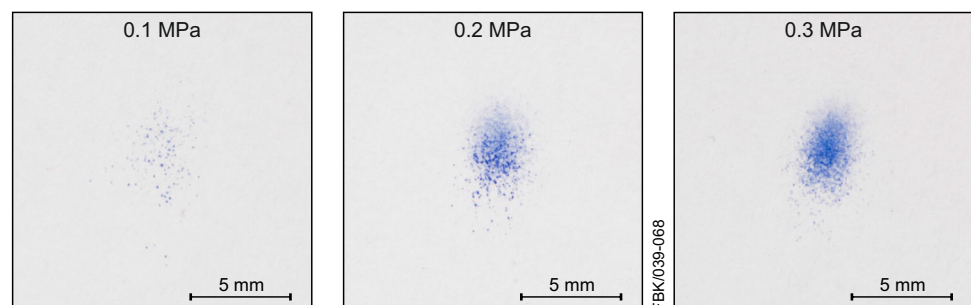
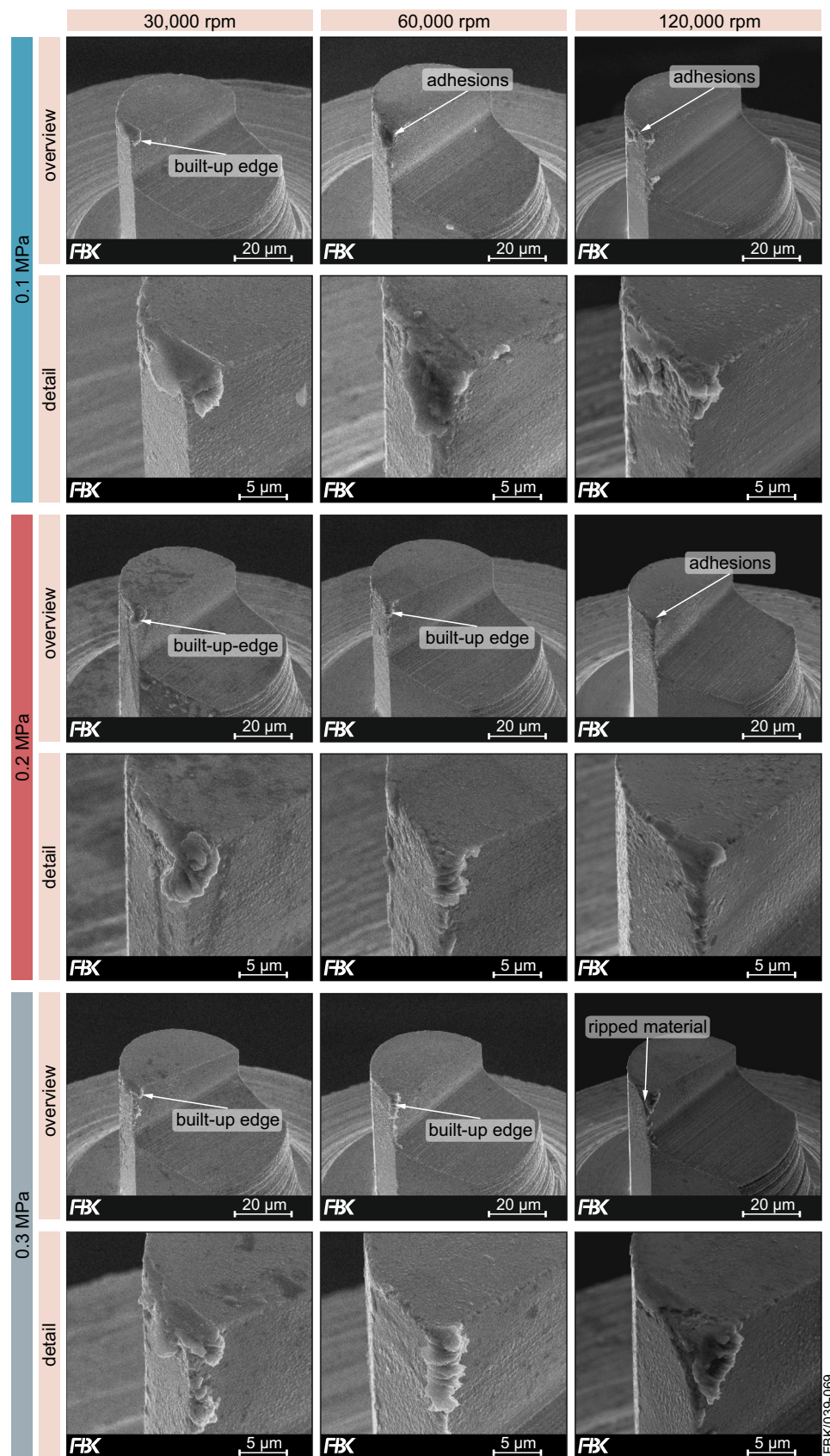


Fig. 8 Wear of micro end mills after a feed travel of 1000 mm depending on air pressure and spindle speed



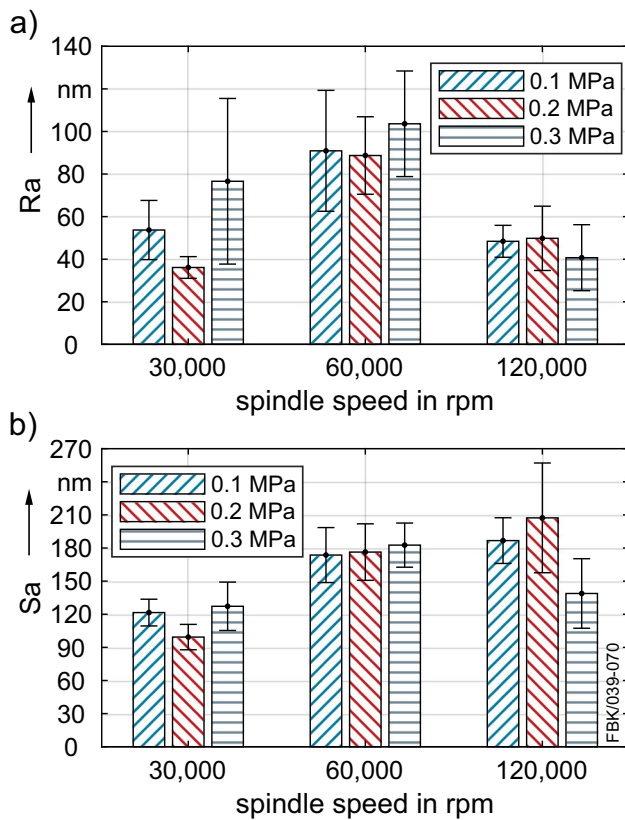


Fig. 9 Surface roughness results depending on air pressure and spindle speed: a) Ra values, and b) Sa values

tent with the SEM images of the tools after micro milling, which show built-up edges for both parameter combinations. Built-up edges also can be seen on the SEM images of the tools, for which only the standard deviation extends beyond $52 \mu\text{m}$.

Figure 10 b) shows the slot depth as a function of spindle speed and air pressure. It shows that almost all mean values are within the range of $4.5 \mu\text{m}$ to $5.5 \mu\text{m}$. Only the mean values of “120,000 rpm-0.1 MPa” ($5.9 \mu\text{m}$) and “60,000 rpm-0.3 MPa” ($5.6 \mu\text{m}$) are outside this range. Analogous to the slot width, this high value can be attributed to built-up edge formation. If a strong built-up edge formation has occurred, it can be presumed that the cooling lubrication was insufficient. Looking at the results of the slot width and depth from this point of view, this means: Cooling lubrication at 30,000 rpm was sufficient at 0.2 MPa and 0.3 MPa. At 60,000 rpm, built-up edge formation could not be completely prevented with any parameter combination. At 120,000 rpm, sufficient cooling lubrication could be achieved at 0.2 MPa. The slightly lower value of $4.7 \mu\text{m} \pm 0.3 \mu\text{m}$ at “120,000 rpm-0.3 MPa” is due to the breakout at the cutting corner.

To summarize, the following results can be noted regarding manufacturing accuracy: With the spindle speed of 30,000 rpm, the best results were obtained at an air pres-

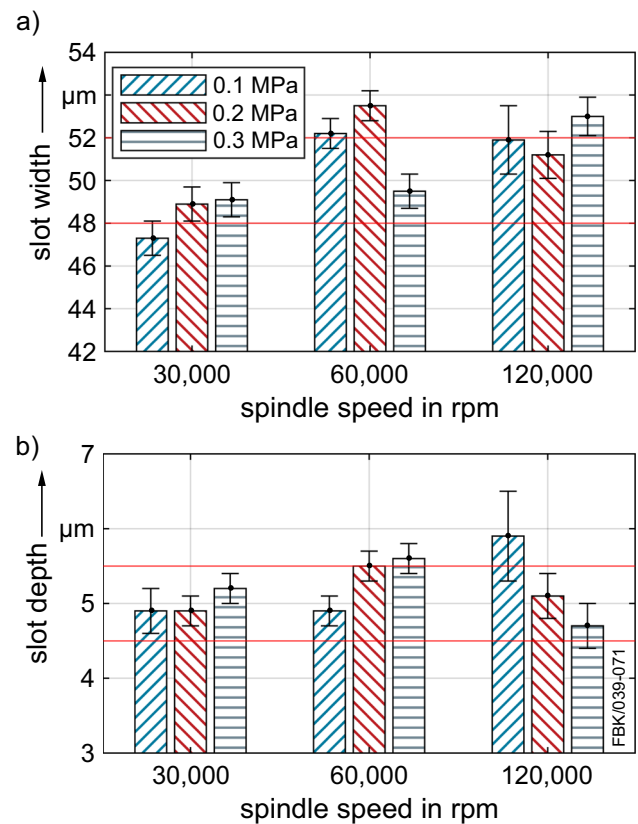


Fig. 10 Manufacturing accuracy results depending on air pressure and spindle speed: a) slot width, and b) slot depth

sure of 0.2 MPa and 0.3 MPa. Concerning the spindle speed of 60,000 rpm no acceptable manufacturing accuracy was achieved with any of the pressures investigated. At the spindle speed 120,000 rpm and an air pressure of 0.2 MPa the best dimensional accuracy was achieved. Maybe too low air pressures do not allow sufficient cooling lubrication of the contact zone, due to the comparably low number of large droplets.

4 Conclusion

In this study the influence of the supply direction (0° , 90° , 180° and 270°) and the air pressure (0.1 MPa, 0.2 MPa and 0.3 MPa) when micro milling under MQL condition on tool wear, surface quality, burr formation and manufacturing accuracy were analyzed.

Concerning the supply direction, the best results were obtained with a supply direction of 180° . With this value, the lowest roughness and the most uniform slot bottom structure were achieved, which indicates better cooling lubrication compared to the other supply directions. Regarding the influence of the supply direction on tool wear, no significant

differences could be found. Based on the results, the 180° supply direction was selected for the further investigations.

With regard to the air pressure, no clear result could be achieved. The influence of the spindle speed on the process results was higher than the influence of the air pressure. However, the following conclusions can be drawn: With the spindle speed of 30,000 rpm, the best results were obtained at an air pressure of 0.2 MPa. No statement can be done concerning the spindle speed of 60,000 rpm: while here the lowest roughness values resulted for 0.1 MPa and 0.2 MPa, no acceptable manufacturing accuracy was achieved with any of the pressures investigated. At the spindle speed 120,000 rpm and an air pressure of 0.2 MPa, a slightly worse roughness was achieved compared to 0.1 MPa, but the dimensional accuracy is better. When using 0.3 MPa at 120,000 rpm, tool breakage occurred after a feed travel of 550 mm or 150 mm for two of the three tools, respectively. This leads to the conclusion that this combination can be classified as unsuitable and should be avoided. Although no obvious best air pressure could be identified, better results tended to be obtained for 0.2 MPa. A reason for this could be that too low pressures are not sufficient to assure the supply of the MWF to the contact zone, and if the pressure is too high, the softened material cools down too quickly on the tool, leading to breakouts or tool fractures caused by too large built-up edges.

In future investigations, different MWFs will be supplied under MQL condition during micro milling to identify their impact on the process results. In addition, wet machining and dry machining will be compared to MQL.

Author contribution All authors contributed to the study conception and design. Execution of experiments, data collection and analysis were performed by Sonja Kieren-Ehse and Tobias Mayer. The first draft of the manuscript was written by Sonja Kieren-Ehse and all authors commented on previous versions of the manuscript. All authors read and approved the final manuscript.

Funding Funded by the Deutsche Forschungsgemeinschaft (DFG, German Research Foundation) –Project-ID 172116086–SFB 926. Open Access funding enabled and organized by Projekt DEAL.

Declaration

Competing interests The authors declare no competing interests.

Open Access This article is licensed under a Creative Commons Attribution 4.0 International License, which permits use, sharing, adaptation, distribution and reproduction in any medium or format, as long as you give appropriate credit to the original author(s) and the source, provide a link to the Creative Commons licence, and indicate if changes were made. The images or other third party material in this article are included in the article's Creative Commons licence, unless indicated otherwise in a credit line to the material. If material is not included in the article's Creative Commons licence and your intended use is not permitted by statutory regulation or exceeds the permitted use, you will need to obtain permission directly from the copy-

right holder. To view a copy of this licence, visit <http://creativecommons.org/licenses/by/4.0/>.

References

1. Thepsonthi T, Özel T (2012) Multi-objective process optimization for micro-end milling of Ti-6Al-4V titanium alloy. *Int J Adv Manuf Technol* 63(9–12):903–914. <https://doi.org/10.1007/s00170-012-3980-z>
2. Cheng K, Huo D (2013) *Micro-cutting: fundamentals and applications*. Microsystem and Nanotechnology. Chichester West Sussex United Kingdom: Wiley
3. Niu Z, Jiao F, Cheng K (2018) An innovative investigation on chip formation mechanisms in micro-milling using natural diamond and tungsten carbide tools. *J Manuf Process* 31:382–394. <https://doi.org/10.1016/j.jmapro.2017.11.023>
4. Prengel HG, Pfouts WR, Santhanam AT (1998) State of the art in hard coatings for carbide cutting tools. *Surf Coat Technol* 102:183–190
5. Uhlmann E, Oberschmidt D, Kuche Y, Löwenstein A (2014) Cutting edge preparation of micro milling tools. *Procedia CIRP* 14:349–354. <https://doi.org/10.1016/j.procir.2014.03.083>
6. Li KM, Chou SY (2010) Experimental evaluation of minimum quantity lubrication in near micro-milling. *J Mater Process Technol* 210(15):2163–2170. <https://doi.org/10.1016/j.jmatprotec.2010.07.031>
7. Biermann D, Steiner M (2012) Analysis of micro burr formation in austenitic stainless steel X5CrNi18-10. *Procedia CIRP* 3:97–102. <https://doi.org/10.1016/j.procir.2012.07.018>
8. Kakinuma Y, Yasuda N, Aoyama T (2008) Micromachining of soft polymer material applying cryogenic cooling. *J Adv Mech Des Syst Manuf* 2(4):560–569. <https://doi.org/10.1299/jamdsm.2.560>
9. Zainal Abidin Z, Tarisai Mativenga P, Harrison G (2020) Chilled air system and size effect in micro-milling of Nickel–titanium shape memory alloys. *Int J Precis Eng Manuf-Green Technol* 7(2):283–297. <https://doi.org/10.1007/s40684-019-00040-5>
10. Marcon A, Melkote S, Kalaitzidou K, DeBra D (2010) An experimental evaluation of graphite nanoplatelet based lubricant in micro-milling. *CIRP Annals* 59(1):141–144. <https://doi.org/10.1016/j.cirp.2010.03.083>
11. Roushan A, Rao US, Patra K, Sahoo P (2022) Performance evaluation of tool coatings and nanofluid MQL on the micro-machinability of Ti-6Al-4V. *J Manuf Process* 73:595–610. <https://doi.org/10.1016/j.jmapro.2021.11.030>
12. Mittal RK, Kulkarni SS, Singh RK (2017) Effect of lubrication on machining response and dynamic instability in high-speed micromilling of Ti-6Al-4V. *J Manuf Process* 28:413–421. <https://doi.org/10.1016/j.jmapro.2017.04.007>
13. Anand KN, Mathew J (2020) Evaluation of size effect and improvement in surface characteristics using sunflower oil-based MQL for sustainable micro-endmilling of Inconel 718. *J Braz Soc Mech Sci Eng* 42(4):156. <https://doi.org/10.1007/s40430-020-2239-0>
14. Yang X, Cheng X, Li Y, Zheng G, Xu R (2020) Machinability investigation and sustainability analysis of minimum quantity lubrication-assisted micro-milling process. *Proc IME B J Eng Manufact* 234(11):1388–1401. <https://doi.org/10.1177/0954405420921727>
15. Danish M, Aslantas K, Hascelik A, Rubaiee S, Gupta MK, Yildirim MB et al (2022) An experimental investigations on effects of cooling/lubrication conditions in micro milling of additively manufactured Inconel 718. *Tribol Int* 173:107620. <https://doi.org/10.1016/j.triboint.2022.107620>

16. Qu D, Zhang P, Xue J, Fan Y, Chen Z, Wang B (2018) Experimental Study on the effects of coolants on surface quality and mechanical properties of micromilled thin-walled elgiloy. *Materials* 11(9):1497. <https://doi.org/10.3390/ma11091497>
17. Pham MQ, Yoon HS, Khare V, Ahn SH (2014) Evaluation of ionic liquids as lubricants in micro milling - process capability and sustainability. *J Clean Prod* 76:167–173. <https://doi.org/10.1016/j.jclepro.2014.04.055>
18. Zheng X, Liu Z, Chen M, Wang X (2013) Experimental study on micro-milling of Ti6Al4V with minimum quantity lubrication. *Int J Nanomanufacturing* 9(5–6):570. <https://doi.org/10.1504/IJNM.2013.057600>
19. Vazquez E, Gomar J, Ciurana J, Rodríguez CA (2015) Analyzing effects of cooling and lubrication conditions in micromilling of Ti6Al4V. *J Clean Prod* 87:906–913. <https://doi.org/10.1016/j.jclepro.2014.10.016>
20. Kieren-Ehse S, Bohley M, Kirsch B, Aurich JC (2019) Influence of the metal working fluid quantity on process results when micro milling cp-titanium with 50 µm diameter micro end mills. *Proceedings of the 19th international conference of the european society for precision engineering and nanotechnology* pp 400–401
21. Ziberov M, Silva MBd, Jackson M, Hung WNP (2016) Effect of Cutting Fluid on Micromilling of Ti-6Al-4V Titanium Alloy. *Procedia Manufacturing* 5:332–347. <https://doi.org/10.1016/j.promfg.2016.08.029>
22. Aslantas K, Çiçek A (2018) The effects of cooling/lubrication techniques on cutting performance in micro-milling of Inconel 718 superalloy. *Procedia CIRP* 77:70–73. <https://doi.org/10.1016/j.procir.2018.08.219>
23. Hassanpour H, Sadeghi MH, Rezaei H, Rasti A (2016) Experimental Study of Cutting Force, Microhardness, Surface Roughness, and Burr Size on Micromilling of Ti6Al4V in Minimum Quantity Lubrication. *Mater Manuf Process* 31(13):1654–1662. <https://doi.org/10.1080/10426914.2015.1117629>
24. Kim JS, Kim JW, Lee SW (2017) Experimental characterization on micro-end milling of titanium alloy using nanofluid minimum quantity lubrication with chilly gas. *Int J Adv Manuf Technol* 91(5–8):2741–2749. <https://doi.org/10.1007/s00170-016-9965-6>
25. Saha S, Deb S, Bandyopadhyay PP (2021) Progressive wear based tool failure analysis during dry and MQL assisted sustainable micro-milling. *Int J Mech Sci* 212:106844. <https://doi.org/10.1016/j.ijmecsci.2021.106844>
26. Aurich JC, Reichenbach IG, Schüler GM (2012) Manufacture and application of ultra-small micro end mills. *CIRP Annals - Manufacturing Technology*. 61(1):83–86. <https://doi.org/10.1016/j.cirp.2012.03.012>
27. Reichenbach IG, Fallenstein F, Aurich JC (2014) CAE Analysis of Single-Edge Micro End Mills – Methodology and Results. 9th international conference on micro manufacturing. <https://doi.org/10.13140/2.1.1476.4320>
28. Kieren-Ehse S, Mayer T, Kirsch B, Aurich JC (2021) Atomic force microscope for in situ micro end mill characterization - Part I: Integration into a desktop sized machine tool. *Proceedings of the 21th international conference of the european society for precision engineering and nanotechnology* pp 463–466
29. Saha S, Deb S, Bandyopadhyay PP (2022) Shadow zone in MQL application and its influence on lubricant deficiency and machinability during micro-milling. *Int J Mech Sci* 220:107181. <https://doi.org/10.1016/j.ijmecsci.2022.107181>
30. Aslantas K, Hopa HE, Percin M, Çiçek Ucuñ İ, A, (2016) Cutting performance of nano-crystalline diamond (NCD) coating in micro-milling of Ti6Al4V alloy. *Precis Eng* 45:55–66. <https://doi.org/10.1016/j.precisioneng.2016.01.009>
31. Kiswanto G, Zariatin DL, Ko TJ (2014) The effect of spindle speed, feed-rate and machining time to the surface roughness and burr formation of Aluminum Alloy 1100 in micro-milling operation. *J Manuf Process* 16(4):435–450. <https://doi.org/10.1016/j.jmapro.2014.05.003>
32. Xu G (1996) Einfluß der Schneidkantenform auf die Oberflächenausbildung beim Hochgeschwindigkeitsfräsen mit Feinkornhartmetall [Dissertation]. Techn Hochsch Darmstadt Aachen

Publisher's Note Springer Nature remains neutral with regard to jurisdictional claims in published maps and institutional affiliations.